Control and Cybernetics
vol. **23** (1994) No. 3

Axisymmetric thin shell structures sizing and shape optimization

by

C. A. Mota Soares
CEMUL/IST
Av. Rovisco Pais
1096 Lisboa Codex, Portugal

J. Infante Barbosa
ENIDH/DMM
Paço de Arcos
2780 Oeiras, Portugal

and

C. M. Mota Soares
CEMUL/IST
Av. Rovisco Pais
1096 Lisboa Codex, Portugal

The paper presents the structural and the sensitivity analyses for the optimization of axisymmetric shells subject to static and dynamic constraints and arbitrary loading. Thickness and shape design variables are considered. The model is based on a two node frustum conical finite element with 8 degrees of freedom given on Love–Kirchhoff assumptions. The objectives of the design are minimization of the volume of the shell material, maximization of the fundamental natural frequency, minimization of the maximum stresses or the minimization of maximum displacements. The constraint functions are the displacements, stresses, enclosed volume of the structure, volume of shell material or the natural frequency of a specified mode shape. The sensitivities are calculated by analytical, semi–analytical and global finite difference techniques. The efficiency and accuracy of the models developed are discussed with reference to applications.

1. Introduction

Structural optimization using finite element techniques requires sequential use of structural and sensitivity analyses combined with a numerical optimizer. The success of the structural optimization process depends on the proper choices with

respect to the finite element model, sensitivity analysis, objective function, constraints, design variables and method of solution of the nonlinear mathematical problem.

This work presents a frustum–cone finite element model with 8 degrees of freedom, based on Love–Kirchhoff assumptions, for thin axisymmetric shell structures (Zienkiewicz, 1977). The sensitivities with respect to the design variables, the thicknesses and/or radial nodal coordinates, are evaluated analytically, semi–analytically or by finite difference.

The evaluation of sensitivities of structural response to changes in design variables is a crucial stage in the optimal design of complex structures, representing a major factor with regard to the computer time required for the optimization process. Hence it is important to have efficient techniques to calculate these derivatives. The simplest technique of evaluating sensitivities of response with respect to changes in design variables is through the finite difference approximation, called here global finite difference, which is computationally expensive, or through the use of semi–analytical method (Zienkiewicz and Campbell, 1973; Cheng and Liu, 1987; Barthelemy et al., 1988) or the analytical method as described in the next sections. These later methods can both be applied with the direct or adjoint structure technique for static type of situations (Haftka and Kamat, 1987).

In this paper the formulation for the sensitivities of axisymmetric shells is presented for the general case of arbitrary loading. Other numerically based solutions are reported by Marcelin and Trompette (1988) using a finite element with a two node straight element and/or a three node parabolic element based on Love–Kirchhoff shell theory associated to the semi–analytical method to evaluate the sensitivities. Others authors, such as Plaut et al. (1984) and Chenais (1987), present alternative theories and models for optimization of shell structures. Mehrez and Rousselet (1989) presented the analysis and optimization of shells of revolution using Koiter's model with the implementation of B–Splines for the middle surface and finite element for displacements. More recently, Bernardou et al. (1991) used only the general continuous formulation of the problems and presented a methodology for optimizing the shape (middle surface and thickness) of an elastic general thin shell under different criteria.

The formulation presented in this paper is applied to the minimum weight design of thin axisymmetric shell structures subject to constraints on displacements, stresses, natural frequencies, volume of the shell material and enclosed volume of the structure. Maximization of the natural frequency of a chosen vibration mode, minimization of maximum displacement or alternatively minimization of maximum stresses using a bound formulation is carried out. A comparative study of analytical versus semi–analytical and global finite difference shows the advantage of analytical sensitivities with regard to the accuracy and the advantage of semi–analytical sensitivities with regard to CPU time.

The ADS (Automated Design Synthesis) program of Vanderplaats (1987) is used to solve the nonlinear mathematical programming problem.

2. Thin axisymmetric shells

Structural analysis of axisymmetric shells using finite element methods requires a discretized model where the complete shell can be idealized as a series of shell ring elements joined at their nodal point circles. Its behaviour will be characterized by the displacements of these nodal circles which are described in terms of a finite number of displacement variables or generalized displacements.

For an arbitrary shell the strain–displacement relations for small displacements in an orthogonal curvilinear system are given (Kraus, 1967) by :

$$\epsilon_i = \frac{\partial}{\partial \alpha_i}\left(\frac{u_i}{\sqrt{g_i}}\right) + \frac{1}{2g_i}\sum_{k=1}^{3}\frac{\partial g_i}{\partial \alpha_k}\frac{u_k}{\sqrt{g_k}} \quad (i=1,2,3) \tag{1}$$

$$\gamma_{ij} = \frac{1}{\sqrt{g_i g_j}}\left[g_i \frac{\partial}{\partial \alpha_j}\left(\frac{u_i}{\sqrt{g_i}}\right) + g_j \frac{\partial}{\partial \alpha_i}\left(\frac{u_j}{\sqrt{g_j}}\right)\right] \quad \begin{pmatrix} i,j=1,2,3; \\ i \neq j \end{pmatrix} \tag{2}$$

where ϵ_i are the normal strains, α_i the curvilinear coordinates, u_i the displacement components, g_i the first fundamental magnitudes and γ_{ij} the shear strains.

Considering the Love–Kirchhoff approximation of the theory of thin elastic shells which is based on the postulate that the shell is thin, the deflections of the shell are small, the transverse normal stress is negligible and normals to the reference surface of the shell remain normal to it and undergo no change in length during deformation. For a conical shell (Fig. 1) represented by its reference surface of revolution, the displacement components are represented as:

$$u_1 = U(S,\theta,\xi); \qquad u_2 = V(S,\theta,\xi); \qquad u_3 = W(S,\theta,\xi)$$

For this particular situation and assuming for thin shells $\xi/R_i \simeq 0$, where $1/R_i$ are the principal curvatures, equations (1) and (2) can be represented as :

$$\begin{aligned}
\epsilon_{SS} &= \frac{\partial U}{\partial S} \\
\epsilon_{\theta\theta} &= \frac{1}{r}\left(\frac{\partial V}{\partial \theta} + U\cos\phi + W\sin\phi\right) \\
\epsilon_{\xi\xi} &= \frac{\partial W}{\partial \xi} \\
\gamma_{S\theta} &= \frac{\partial V}{\partial S} + \frac{1}{r}\left(\frac{\partial U}{\partial \theta} - V\cos\phi\right) \\
\gamma_{S\xi} &= \frac{\partial W}{\partial S} + \frac{\partial U}{\partial \xi} \\
\gamma_{\theta\xi} &= \frac{1}{r}\frac{\partial W}{\partial \theta} + r\frac{\partial}{\partial \xi}\left(\frac{V}{r}\right) \\
U &= U(S,\theta,\xi) \\
V &= V(S,\theta,\xi)
\end{aligned} \tag{3}$$

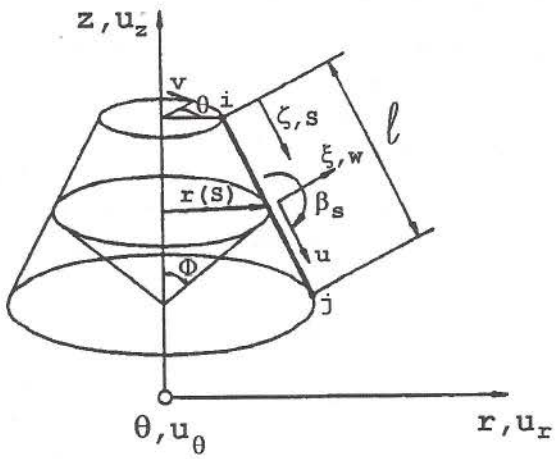

Figure 1. Frustum–cone finite element. Geometry and displacements.

$$W = W(S,\theta,\xi)$$

where U, V, W are the components of the displacement vector of a spatial point and S, θ, ξ are, respectively, the coordinates along the meridian, parallel circle and normal to the reference surface of the shell (Fig. 1).

Assuming the following displacement distribution :

$$\begin{aligned} U(S,\theta,\xi) &= u(S,\theta) + \xi \frac{\partial U}{\partial \xi}|_{\xi=0} \\ V(S,\theta,\xi) &= v(S,\theta) + \xi \frac{\partial V}{\partial \xi}|_{\xi=0} \\ W(S,\theta,\xi) &= w(S,\theta) \end{aligned} \tag{4}$$

where $u(S,\theta)$, $v(S,\theta)$ and $w(S,\theta)$ represent the components of the displacement vector of a point on the reference middle surface of the shell and $\frac{\partial U}{\partial \xi}|_{\xi=0}$ and $\frac{\partial V}{\partial \xi}|_{\xi=0}$ represent, respectively, the rotations of tangents to the reference surface oriented along the lines S and θ. Let $\frac{\partial U}{\partial \xi}|_{\xi=0} = \beta_S(S,\theta)$ and $\frac{\partial V}{\partial \xi}|_{\xi=0} = \beta_\theta(S,\theta)$. Using the Love–Kirchhoff assumptions ($\gamma_{S\xi} = \gamma_{\theta\xi} = 0$), one obtains :

$$\begin{aligned} \beta_S &= -\frac{\partial w}{\partial S} \\ \beta_\theta &= \frac{v}{r}\sin\phi - \frac{1}{r}\frac{\partial w}{\partial \theta} \end{aligned} \tag{5}$$

The displacement vector $\underline{U} = [U\ V\ W]^T$ of a given point (S,θ,ξ) can be expressed in terms of the displacement vector $\mathsf{U} = [u,v,w]^T$ of the reference

surface and the rotations of tangents (β_S, β_θ) of the same reference surface oriented along the parametric lines as :

$$\underline{U} = \begin{bmatrix} u \\ v \\ w \end{bmatrix} + \begin{bmatrix} \xi & 0 \\ 0 & \xi \\ 0 & 0 \end{bmatrix} \begin{bmatrix} \beta_S \\ \\ \beta_\theta \end{bmatrix} \tag{6}$$

Substituting relations (6) into the remainder of equations (3), the non– vanishing strains in the thin elastic shell are given by:

$$\epsilon = \epsilon^\circ + \xi\chi \tag{7}$$

with: $\epsilon = [\epsilon_{SS}\ \epsilon_{\theta\theta}\ \gamma_{S\theta}]^T$; $\epsilon^\circ = [\epsilon^\circ_{SS}\ \epsilon^\circ_{\theta\theta}\ \gamma^\circ_{S\theta}]^T$; $\chi = [\chi_{SS}\ \chi_\theta\ \chi_{S\theta}]^T$ and:

$$\epsilon^\circ = \Delta_m \mathsf{U} \tag{8}$$

$$\chi = \Delta_f \mathsf{U} \tag{9}$$

where the operators Δ_m and Δ_f are, respectively:

$$\Delta_m = \begin{bmatrix} \frac{\partial}{\partial S} & 0 & 0 \\ \frac{\cos\phi}{r} & \frac{1}{r}\frac{\partial}{\partial\theta} & \frac{\sin\phi}{r} \\ \frac{1}{r}\frac{\partial}{\partial\theta} & \left(\frac{\partial}{\partial S} - \frac{\cos\phi}{r}\right) & 0 \end{bmatrix}$$

$$\Delta_f = \begin{bmatrix} 0 & 0 & -\frac{\partial^2}{\partial S^2} \\ 0 & \frac{\sin\phi}{r^2}\frac{\partial}{\partial\theta} & -\frac{1}{r^2}\left(\frac{\partial^2}{\partial\theta^2} + r\cos\theta\frac{\partial}{\partial S}\right) \\ 0 & \frac{2\sin\phi}{r^2}\left(r\frac{\partial}{\partial S} - \cos\phi\right) & \frac{2}{r^2}\left(\cos\phi\frac{\partial}{\partial\theta} - r\frac{\partial^2}{\partial S\partial\theta}\right) \end{bmatrix}$$

The quantities ϵ°_{SS}, $\epsilon^\circ_{\theta\theta}$, $\gamma^\circ_{S\theta}$ represent, respectively, the meridional, circumferential and shearing strains of the reference surface. The quantities χ_{SS} and $\chi_{\theta\theta}$ represent the changes in the curvature of the reference surface and $\chi_{S\theta}$ represents the torsion of the same surface during deformation.

Assume that the displacements u, v, w can be expanded in Fourier series of the type :

$$\mathsf{U} = \sum_{n=0}^{N} (\mathbb{C}_n \mathsf{U}_n + \hat{\mathbb{C}}_n \hat{\mathsf{U}}_n) \tag{10}$$

where:

$$\mathbb{C}_n = \begin{bmatrix} \cos n\theta & 0 & 0 \\ 0 & \sin n\theta & 0 \\ 0 & 0 & \cos n\theta \end{bmatrix}; \qquad \hat{\mathbb{C}}_n = \begin{bmatrix} \sin n\theta & 0 & 0 \\ 0 & \cos n\theta & 0 \\ 0 & 0 & \sin n\theta \end{bmatrix}$$

$$\mathsf{U}_n = [u_n\ v_n\ w_n]^T; \qquad \hat{\mathsf{U}}_n = [\hat{u}_n\ \hat{v}_n\ \hat{w}_n]^T$$

The first and second terms of equation (10) represent these components of displacements which are, respectively, symmetric and antisymmetric with respect to the plane passing through $\theta = 0$ and z, u_n, v_n and w_n being the amplitudes of symmetric part and $\hat{u}_n$, $\hat{v}_n$ and $\hat{w}_n$ the amplitudes of antisymmetric part for the nth harmonic and N is the number of terms in the truncated Fourier series.

Since the angular dependence of displacement components is expressed in terms of trigonometric functions, the orthogonality properties of such functions yield a formulation of the problem as a series of uncoupled quasi two–dimensional problems, in which the displacement amplitudes u_n, v_n, w_n, $\hat{u}_n$, $\hat{v}_n$ and $\hat{w}_n$ are the unknowns. The meridional dependence of these displacements amplitudes along the frustum cone represented here only by the symmetric part, can for the sake of simplicity, be assumed as:

$$\mathsf{U}_n = \mathbb{N} q^l_{e_n} \tag{11}$$

where:

$$\mathbb{N} = \begin{bmatrix} N_1 & 0 & 0 & 0 & N_2 & 0 & 0 & 0 \\ 0 & N_1 & 0 & 0 & 0 & N_2 & 0 & 0 \\ 0 & 0 & N_3 & N_4 & 0 & 0 & N_2 & N_6 \end{bmatrix}; \tag{12}$$

$$\begin{aligned} N_1 &= (1-\zeta) \\ N_2 &= \zeta \\ N_3 &= (1-3\zeta^2+2\zeta^3) \\ N_4 &= (\zeta-2\zeta^2+\zeta^3)\ell \\ N_5 &= (3\zeta^2-2\zeta^3) \\ N_6 &= (-\zeta^2+\zeta^3)\ell \end{aligned}$$

$$q^l_{e_n} = \left[u^i_n \;\; v^i_n \;\; w^i_n \;\; \frac{dw^i_n}{dS} \;\; u^j_n \;\; v^j_n \;\; w^j_n \;\; \frac{dw^j_n}{dS} \right]^T$$

$$\ell = \sqrt{(r^j - r^i)^2 + (z^j - z^i)^2}; \quad r = (1-\zeta)\, r^i + \zeta r^j; \quad \zeta = \frac{S}{\ell}$$

$\mathbb{N}$ being the matrix of shape functions, $q^l_{e_n}$ the vector of displacement amplitude components in local coordinates, ℓ the length of the frustum–cone element, r^i and r^j the radial coordinates of nodes i and j and S the coordinate over the length of the frustum–cone element (Fig. 1).

Substitution of equations (10) and (11) into equation (8) yields for the nth harmonic:

$$\epsilon_{m_n} = B^*_{m_n} q^l_{e_n} \tag{13}$$

where

$$\epsilon_{m_n} = \begin{bmatrix} \epsilon^0_{SS_n} \\ \epsilon^0_{\theta\theta_n} \\ \gamma^0_{S\theta_n} \end{bmatrix}; \quad B^*_{m_n} = \begin{bmatrix} B_{11} & 0 & 0 & 0 & -B_{11} & 0 & 0 & 0 \\ B_{21} & B_{22} & B_{23} & B_{24} & B_{25} & B_{26} & B_{27} & B_{28} \\ B_{31} & B_{32} & 0 & 0 & B_{35} & B_{36} & 0 & 0 \end{bmatrix} \tag{14}$$

$\epsilon^0_{SS_n}$, $\epsilon^0_{\theta\theta_n}$ and $\gamma^0_{S\theta_n}$ representing, respectively, the amplitudes for the nth harmonic of the meridional, circumferential and shearing strains of the reference surface. The $B^*_{m_n}$ are derived by applying the strain operator Δ_m to the displacement shape functions yielding:

$$\begin{aligned}
B_{11} &= -\tfrac{1}{\ell}\cos n\theta; & B_{21} &= \tfrac{N_1}{r}\cos\phi\cos n\theta;\\
B_{22} &= \tfrac{N_1}{r}n\cos n\theta; & B_{23} &= \tfrac{N_3}{r}\sin\phi\cos n\theta;\\
B_{24} &= \tfrac{N_4}{r}\sin\phi\cos n\theta; & B_{25} &= \tfrac{N_2}{r}\cos\phi\cos n\theta;\\
B_{26} &= \tfrac{N_2}{r}n\cos n\theta; & B_{27} &= \tfrac{N_5}{r}\sin\phi\cos n\theta;\\
B_{28} &= \tfrac{N_6}{r}\sin\phi\cos n\theta; & B_{31} &= -\tfrac{N_1}{r}n\sin n\theta;\\
B_{35} &= -\tfrac{N_2}{r}n\sin n\theta; & B_{32} &= -\left(\tfrac{1}{\ell}+\tfrac{N_1}{r}\cos\phi\right)\sin n\theta;\\
B_{36} &= \left(\tfrac{1}{\ell}-\tfrac{N_2}{r}\cos\phi\right)\sin n\theta
\end{aligned} \tag{15}$$

Considering the transformation matrix L relating nodal local coordinates (S,θ,ξ) to nodal global coordinates (r,θ,z) (Fig. 1), one obtains the relationship between the displacements amplitudes in the local referential $(q^l_{e_n})$ and the displacement amplitudes in the global referential (q_{e_n}):

$$q^l_{e_n} = L q_{e_n} \tag{16}$$

where :

$$q_{e_n} = \left[u^i_{r_n}\ \ u^i_{z_n}\ \ u^i_{\theta_n}\ \ \frac{dw^i_n}{dS}\ \ u^j_{r_n}\ \ u^j_{z_n}\ \ u^j_{\theta_n}\ \ \frac{dw^j_n}{dS}\right]^T$$

$$L = \begin{bmatrix} \begin{bmatrix} A \end{bmatrix} & \begin{bmatrix} 0 \end{bmatrix} \\ \begin{bmatrix} 0 \end{bmatrix} & \begin{bmatrix} A \end{bmatrix} \end{bmatrix}$$

$$\begin{bmatrix} A \end{bmatrix} = \begin{bmatrix} \cos\phi & -\sin\phi & 0 & 0 \\ 0 & 0 & 1 & 0 \\ \sin\phi & \cos\phi & 0 & 0 \\ 0 & 0 & 0 & 1 \end{bmatrix}; \quad \begin{bmatrix} 0 \end{bmatrix} = \begin{bmatrix} 0 & 0 & 0 & 0 \\ 0 & 0 & 0 & 0 \\ 0 & 0 & 0 & 0 \\ 0 & 0 & 0 & 0 \end{bmatrix}$$

Substituting equation (16) into the strain–displacement relation (Eq. 13), one obtains the membrane terms of the strain–displacement in terms of the element degrees of freedom of the nth harmonic as:

$$\epsilon_{m_n} = B_{m_n} q_{e_n} \tag{17}$$

where:

$$B_{m_n} = B^{\star}_{m_n} L \tag{18}$$

For the bending terms the procedure is identical, yielding:

$$\chi_{f_n} = B^{*}_{f_n} q^{l}_{e_n} \tag{19}$$

where :

$$\chi_{f_n} = \begin{bmatrix} \chi_{SS_n} \\ \chi_{\theta\theta_n} \\ \chi_{S\theta_n} \end{bmatrix}; \quad B^{*}_{f_n} = \begin{bmatrix} 0 & 0 & \mathbb{B}_{13} & \mathbb{B}_{14} & 0 & 0 & -\mathbb{B}_{13} & \mathbb{B}_{18} \\ 0 & \mathbb{B}_{22} & \mathbb{B}_{23} & \mathbb{B}_{24} & 0 & \mathbb{B}_{26} & \mathbb{B}_{27} & \mathbb{B}_{28} \\ 0 & \mathbb{B}_{32} & \mathbb{B}_{33} & \mathbb{B}_{34} & 0 & \mathbb{B}_{36} & \mathbb{B}_{37} & \mathbb{B}_{38} \end{bmatrix}$$

and:

$$\begin{aligned}
\mathbb{B}_{13} &= \tfrac{6-12\zeta}{\ell^2}\cos n\theta; \\
\mathbb{B}_{14} &= \tfrac{4-6\zeta}{\ell}\cos n\theta; \\
\mathbb{B}_{18} &= \tfrac{2-6\zeta}{\ell}\cos n\theta; \\
\mathbb{B}_{22} &= \tfrac{N_1 n \sin\phi}{r^2}\cos n\theta; \\
\mathbb{B}_{23} &= \left(\tfrac{n^2 N_3}{r^2} + \tfrac{\cos\phi(6\zeta-6\zeta^2)}{\ell r}\right)\cos n\theta; \\
\mathbb{B}_{24} &= \left(\tfrac{n^2 N_4}{r^2} + \tfrac{(-1+4\zeta-3\zeta^2)\cos\phi}{r}\right)\cos n\theta; \\
\mathbb{B}_{26} &= \tfrac{N_2 n \sin\phi}{r^2}\cos n\theta; \\
\mathbb{B}_{27} &= \left(\tfrac{n^2 N_5}{r^2} - \tfrac{(6\zeta-6\zeta^2)\cos\phi}{\ell r}\right)\cos n\theta; \\
\mathbb{B}_{28} &= \left(\tfrac{n^2 N_6}{r^2} + \tfrac{(2\zeta-3\zeta^2)\cos\phi}{r}\right)\cos n\theta; \\
\mathbb{B}_{32} &= \left(-\tfrac{2\sin\phi}{r\ell} - \tfrac{2N_1\cos\phi\sin\phi}{r^2}\right)\sin n\theta; \\
\mathbb{B}_{33} &= \left(-\tfrac{2nN_3\cos\phi}{r^2} - \tfrac{2n(6\zeta-6\zeta^2)}{\ell r}\right)\sin n\theta; \\
\mathbb{B}_{36} &= \left(\tfrac{2\sin\phi}{r\ell} - \tfrac{2N_2\sin\phi\cos\phi}{r^2}\right)\sin n\theta; \\
\mathbb{B}_{34} &= \left(-\tfrac{2nN_4\cos\phi}{r^2} + \tfrac{2n(1-4\zeta+3\zeta^2)}{r}\right)\sin n\theta; \\
\mathbb{B}_{37} &= \left(\tfrac{2n(6\zeta-6\zeta^2)}{r\ell} - \tfrac{2nN_5\cos\phi}{r^2}\right)\sin n\theta; \\
\mathbb{B}_{38} &= \left(\tfrac{2n(-2\zeta+3\zeta^2)}{r} - \tfrac{2nN_6\cos\phi}{r^2}\right)\sin n\theta;
\end{aligned}$$

Similarly if one considers the transformation of coordinates (L) of the local referential (S,θ,ξ) to the global referential (r,θ,z), the changes of curvatures for the nth harmonic can be represented as :

$$\chi_{f_n} = B_{f_n} q_{e_n} \tag{20}$$

where :

$$B_{f_n} = B^{*}_{f_n} L \tag{21}$$

The constitutive equation for a linear elastic solid, considering infinitesimal deformation and orthotropic materials, can be written as :

$$\underline{\tau} = \underline{\mathcal{D}\epsilon} \tag{22}$$

where:

$$\underline{\tau} = [\sigma_{SS} \;\; \sigma_{\theta\theta} \;\; \sigma_{\xi\xi} \;\; \sigma_{S\theta} \;\; \sigma_{S\xi} \;\; \sigma_{\theta\xi}]^T$$

$$\underline{\epsilon} = [\epsilon_{SS} \;\; \epsilon_{\theta\theta} \;\; \epsilon_{\xi\xi} \;\; \gamma_{S\theta} \;\; \gamma_{S\xi} \;\; \gamma_{\theta\xi}]^T$$

and $\underline{\mathcal{D}}$ is the constitutive matrix for the three–dimensional linear elastic solid.

As a consequence of the Love theory expressed by $\gamma_{S\xi} = \gamma_{\theta\xi} = \epsilon_{\xi\xi} = \sigma_{\xi\xi} = 0$, the system of stress–strain relations for thin orthotropic axisymmetric shells can be reduced to:

$$\tau = \mathcal{D}\epsilon \tag{23}$$

where:

$$\tau = [\sigma_{SS} \;\; \sigma_{\theta\theta} \;\; \sigma_{S\theta}]^T$$

$$\mathcal{D} = \begin{bmatrix} E_S^* & \nu_{\theta S} E_S^* & 0 \\ \nu_{S\theta} E_\theta^* & E_\theta^* & 0 \\ 0 & 0 & G_{S\theta} \end{bmatrix}$$

$$E_\theta^* = \frac{E_\theta}{1 - \nu_{S\theta}\nu_{\theta S}}; \quad E_S^* = \frac{E_S}{1 - \nu_{S\theta}\nu_{\theta S}}$$

where E_S, E_θ, $G_{S\theta}$, $\nu_{S\theta}$, $\nu_{\theta S}$ are Young's moduli, shear modulus and Poisson's ratio for the material referred to the S and θ directions. Substitution of equations (7) in equations (23) yields :

$$\tau = \mathcal{D}\epsilon^0 + \xi\mathcal{D}\chi \tag{24}$$

Integrating the stress distribution across the thickness of the shell by neglecting $\xi/R \simeq 0$ one obtains:

$$\tau = \frac{1}{h}\mathcal{N} + \xi\frac{12}{h^3}\mathcal{M} \tag{25}$$

where:

$$\mathcal{N} = [\mathcal{N}_{SS} \;\; \mathcal{N}_{\theta\theta} \;\; \mathcal{N}_{S\theta}]^T \quad \text{(membrane resultants)}$$

$$\mathcal{M} = [\mathcal{M}_{SS} \;\; \mathcal{M}_{\theta\theta} \;\; \mathcal{M}_{S\theta}]^T \quad \text{(bending moments)}$$

and:

$$\mathcal{N} = \int_{-h/2}^{h/2} \tau d\xi = D_m \sum_{n=0}^{N} \epsilon_{m_n} \tag{26}$$

$$\mathcal{M} = \int_{-h/2}^{h/2} \tau \xi d\xi = D_f \sum_{n=0}^{N} \chi_{f_n} \tag{27}$$

where D_m and D_f are the membrane and bending constitutive matrices given by:

$$D_m = h\mathcal{D}; \quad D_f = \frac{h^3}{12}\mathcal{D}$$

The kinetic energy T^e of the eth element is given by the expression:

$$T^e = \frac{1}{2}\int_\Omega \varrho \dot{\underline{U}}^T \dot{\underline{U}} d\Omega = \frac{1}{2}\int_0^{2\pi}\int_0^1\int_{-h/2}^{h/2} \varrho \dot{\underline{U}}^T \dot{\underline{U}} \ell r d\xi d\zeta d\theta \tag{28}$$

where $\dot{\underline{U}} = d\underline{U}/dt$, $d\Omega$ is the elementary volume and is the mass per unit of volume. Substituting equation (5) into equation (6) and integrating over the thickness of the element one obtains:

$$T^e = \frac{1}{2}\varrho \int_0^{2\pi}\int_0^1 h\dot{\underline{U}}^T \dot{\underline{U}} \ell r d\zeta d\theta + \frac{1}{2}\frac{\varrho}{12}\int_0^{2\pi}\int_0^1 h^3 \dot{\kappa}^T \dot{\kappa} \ell r d\zeta d\theta \tag{29}$$

where:

$$\dot{\underline{U}} = \frac{d}{dt}[u \;\; v \;\; w]^T$$

$$\dot{\kappa} = \frac{d}{dt}[-\frac{\partial w}{\partial S} \;\; \frac{1}{r}\left(v\sin\phi - \frac{\partial w}{\partial \theta}\right) \;\; 0]^T$$

In equation (29) the first term represents the translational kinetic inertia and the second term represents the rotational kinetic inertia. It is important to take note that the coupled terms of Fourier series of the type $(\sin m\theta \; \sin n\vartheta)$ and $(\cos m\theta \; \cos n\theta)$ for $m \neq n$ are not considered by making use of the orthogonality of the harmonic functions in the interval $0 \leq \theta \leq 2\pi$ and because the thickness is assumed uniform along θ those terms are equal to zero, resulting for the integration in θ:

$$\begin{array}{lll} \int_0^{2\pi} \cos n\theta \cos m\theta d\theta = \mathcal{A}_1 & \mathcal{A}_1 = \mathcal{A}_2 = 0 & \text{for } m \neq n \\ \int_0^{2\pi} \cos n\theta \sin m\theta d\theta = 0 & \mathcal{A}_1 = 2\pi; \quad \mathcal{A}_2 = 0 & \text{for } m = n = 0 \\ \int_0^{2\pi} \sin n\theta \sin m\theta d\theta = \mathcal{A}_2 & \mathcal{A}_1 = \mathcal{A}_2 = \pi & \text{for } m = n > 0 \end{array} \tag{30}$$

Substituting equations (6), (10) and (11) in the equation (29) for the frustum–cone finite element one obtains :

$$\begin{aligned} T^e = \frac{1}{2}\varrho \sum_{n=0}^{N}\int_0^{2\pi}\int_0^1 h(\mathbb{N}_n L\dot{q}_{e_n})^T(\mathbb{N}_n L\dot{q}_{e_n})\ell r d\zeta d\theta + \\ + \frac{1}{2}\frac{\varrho}{12}\sum_{n=0}^{N}\int_0^{2\pi}\int_0^1 h^3(R_n L\dot{q}_{e_n})^T(R_n L\dot{q}_{e_n})\ell r d\zeta d\theta \end{aligned} \tag{31}$$

where:

$$\dot{q}_{e_n} = \frac{d}{dt} q_{e_n}; \quad \mathbb{N}_n = \mathbb{C}_n \mathbb{N} \text{ and } R_n = \mathbb{C}_n R_n^*$$

in which:

$$R_n^* = \begin{bmatrix} 0 & 0 & -\frac{\partial N_3}{\partial S} & -\frac{\partial N_4}{\partial S} & 0 & 0 & -\frac{\partial N_5}{\partial S} & -\frac{\partial N_6}{\partial S} \\ 0 & \frac{N_1}{r}\sin\phi & \frac{nN_3}{r} & \frac{n\ell N_4}{r} & 0 & \frac{N_2}{r}\sin\phi & \frac{nN_5}{r} & \frac{n\ell N_6}{r} \\ 0 & 0 & 0 & 0 & 0 & 0 & 0 & 0 \end{bmatrix}$$

The kinetic energy can be represented in a simplified form as:

$$T^e = \frac{1}{2}\sum_{n=0}^{N} \left(\dot{q}_{e_n}^T \left(M_{n_T}^e + M_{n_R}^e \right) \dot{q}_{e_n} \right) = \frac{1}{2}\sum_{n=0}^{N} \left(\dot{q}_{e_n}^T M_n^e \dot{q}_{e_n} \right) \tag{32}$$

where M_n^e is the element mass matrix for the nth harmonic represented by:

$$M_n^e = \varrho \int_0^{2\pi}\int_0^1 h(\mathbb{N}_n L)^T (\mathbb{N}_n L) \ell r d\zeta d\theta + \\ + \frac{\varrho}{12}\int_0^{2\pi}\int_0^1 h^3 (R_n L)^T (R_n L) \ell r d\zeta d\theta \tag{33}$$

The element mass matrices M_n^e are full (8×8) matrices which are evaluated taking into consideration the orthogonality properties of the trigonometric functions (Eq. 30).

The strain energy of the eth element is represented by the expression:

$$E^e = \frac{1}{2}\int_\Omega \tau^T \epsilon d\Omega = \frac{1}{2}\int_0^{2\pi}\int_0^1\int_{-h/2}^{h/2} \epsilon^T \mathcal{D} \epsilon r \ell d\xi d\zeta d\theta \tag{34}$$

Introducing equation (7) in the above equation and taking advantage of the orthogonality properties of the trigonometric functions one obtains:

$$E^e = \frac{1}{2}\sum_{n=0}^{N} q_{e_n}^T K_n^e q_{e_n} \tag{35}$$

with:

$$K_n^e = K_{m_n}^e + K_{f_n}^e \tag{36}$$

$$K_{m_n}^e = \int_0^{2\pi}\int_0^1 B_{m_n}^T D_m B_{m_n} r \ell d\zeta d\theta \tag{37}$$

$$K_{f_n}^e = \int_0^{2\pi}\int_0^1 B_{f_n}^T D_f B_{f_n} r \ell d\zeta d\theta \tag{38}$$

where $K_{m_n}^e$ and $K_{f_n}^e$ are the membrane and bending terms of the element stiffness matrix for the nth harmonic. These matrices are evaluated analytically

in the θ direction taking into consideration the orthogonality properties of the trigonometric functions (Eq. 30). In the ζ direction the integration is carried out by Gaussian Quadrature formulae.

Expanding the surface loads $\underline{p} = [p_u \;\; p_\theta \;\; p_w]^T$ in Fourier series, one obtains external work in the form of:

$$W^e = \int_0^{2\pi} \int_0^1 U^T \underline{p} r \ell d\zeta d\theta \tag{39}$$

where:

$$\underline{p} = \sum_{n=0}^{N} \mathbb{C}_n \underline{p}^n; \quad \underline{p}^n = [p_u^n \;\; p_\theta^n \;\; p_w^n]^T$$

Assuming a linear dependence between the above magnitudes of the forces vector and the components of this vector on the nodes of the frustum-cone finite element, one obtains:

$$\underline{p}^n = \mathfrak{N} p_{e_n}^l \tag{40}$$

where :

$$p_{e_n}^l = [p_{u_i}^n \;\; p_{\theta_i}^n \;\; p_{w_i}^n \;\; M_i^n \;\; p_{u_j}^n \;\; p_{\theta_j}^n \;\; p_{w_j}^n \;\; M_j^n]^T$$

$$\mathfrak{N} = \begin{bmatrix} N_1 & 0 & 0 & 0 & N_2 & 0 & 0 & 0 \\ 0 & N_1 & 0 & 0 & 0 & N_2 & 0 & 0 \\ 0 & 0 & N_1 & 0 & 0 & 0 & N_2 & 0 \end{bmatrix} \tag{41}$$

Considering equations (6), (10), (11) and (16) and substituting in equation (39) one gets:

$$W^e = \sum_{n=0}^{N} \int_0^{2\pi} \int_0^1 \left((\mathbb{C}_n \mathbb{N} L q_{e_n})^T \mathbb{C}_n \mathfrak{N} p_{e_n}^l \right) r \ell d\zeta d\theta \tag{42}$$

Using $\mathbb{N}_n = \mathbb{C}_n \mathbb{N}$, making $\mathfrak{N}_n = \mathbb{C}_n \mathfrak{N}$ and $f_n^e = \mathfrak{N}_n p_{e_n}^l$ and using the assumption of orthogonality of the trigonometric functions on the interval $0 \leq \theta \leq 2\pi$, yields:

$$W^e = \sum_{n=0}^{N} q_{e_n}^T p_n^e \tag{43}$$

where :

$$p_n^e = \int_0^{2\pi} \int_0^1 L^T \mathbb{N}_n^T f_n^e r \ell d\zeta d\theta \tag{44}$$

is the load vector of the element for the nth harmonic which is consistent with the assumed displacement field used in deriving mass and stiffness matrices.

Vectors p_n^e are evaluated analytically in the θ direction taking into consideration the orthogonality properties of the trigonometric functions. In the ζ direction the integration may be carried out by Gaussian Quadrature formulae or alternatively by using a symbolic manipulator.

Problems of static equilibrium are governed by the variational principles for the minimum total potential energy, while the dynamic equilibrium is simply formulated in terms of Hamilton's variational principle. Then defining a Lagrangian function through the expression :

$$\mathcal{L} = T^e - \mathbf{V}^e \tag{45}$$

with:

$$\mathbf{V}^e = E^e - \mathbf{W}^e \tag{46}$$

and substituting the values of T^e, E^e and $\mathbf{W}^e$ given by the equations (32), (35) and (43) in the Lagrangian function $\mathcal{L}$, one obtains:

$$\mathcal{L} = \sum_{n=0}^{N} \left(\frac{1}{2} \left(\dot{q}_{e_n}^T M_n^e \dot{q}_{e_n} - q_{e_n}^T K_n^e q_{e_n} \right) + q_{e_n}^T p_n^e \right) \tag{47}$$

Applying the appropriate Lagrange equations of motion for equilibrium yields for the element and for the nth harmonic:

$$M_n^e \ddot{q}_{e_n} + K_n^e q_{e_n} = p_n^e \tag{48}$$

where:

$$\ddot{q}_{e_n} = \frac{d^2(q_{e_n})}{dt^2}$$

For the system these equations become:

$$M\ddot{q} + Kq = p \tag{49}$$

where M, K, q and p are, respectively, the mass and stiffness matrices, the displacement vector and the load vector of the nth harmonic.

Assuming free undamped vibrations, the static and dynamic equilibrium equations for the nth harmonic can be represented symbolically, respectively, as:

$$Kq = p \tag{50}$$

$$Kq = \omega^2 Mq \tag{51}$$

where ω is the natural frequency.

3. Sensitivity analysis

A typical optimization constraint such as a limit on a displacement, stress component or effective stress can be represented by:

$$g_j = g_j(q; b) \leq 0 \tag{52}$$

where b is the vector of design variables and $j \in (1, \ldots, m)$, m being the number of constraints. Thus the sensitivity of the constraint g_j is given by:

$$\frac{dg_j}{db_i} = \frac{\partial g_j}{\partial b_i} + z_j^T \frac{dq}{db_i} \tag{53}$$

where :

$$z_j = \frac{\partial g_j}{\partial q} \tag{54}$$

is the vector of adjoint forces.

For static constraints, the sensitivities are evaluated through the method of the adjoint structure where a virtual structure is defined that satisfies the equilibrium equation:

$$K\lambda_j = z_j \tag{55}$$

with λ_j being the system adjoint degrees of freedom for the constraint g_j. The solution of the system equation (55) gives λ_j. It should be noted that the adjoint structure is identical to the real structure, but subject to a different load. To increase computational efficiency, the already factorized form of the stiffness matrix should be used. Considering the static equilibrium equations (50) and differentiating these with respect to a design variable b_i yields:

$$K\frac{dq}{db_i} = \frac{\partial p}{\partial b_i} - \frac{\partial K}{\partial b_i} q \tag{56}$$

Premultiplying by z_j^T one obtains:

$$z_j^T \frac{dq}{db_i} = z_j^T K^{-1} \left(\frac{\partial p}{\partial b_i} - \frac{\partial K}{\partial b_i} q \right) \tag{57}$$

The inversion of the stiffness matrix K is easily avoided using the adjoint structure method through the solution of equation (55). Thus, the sensitivities given by equation (53) can be evaluated as:

$$\frac{dg_j}{db_i} = \frac{\partial g_j}{\partial b_i} + \lambda_j^T \left(\frac{\partial p}{\partial b_i} - \frac{\partial K}{\partial b_i} q \right) \tag{58}$$

where $\partial K/\partial b_i$ is the sensitivity of the system stiffness matrix and $\partial p/\partial b_i$ is the sensitivity of the system load vector. When the forces are independent of

the design variables the sensitivity of the system load vector is zero and then equation (58) simplifies to:

$$\frac{dg_j}{db_i} = \frac{\partial g_j}{\partial b_i} - \lambda_j^T \frac{\partial K}{\partial b_i} q \tag{59}$$

The term $\partial g_j / \partial b_i$ is usually zero or can easily be obtained.

For dynamics, considering the mode of vibration q_k which corresponds to the natural frequency ω_k, the eigenvalue problem, equation (51), is represented for the system as:

$$K q_k = \omega_k^2 M q_k. \tag{60}$$

Differentiating the above equation with respect to a design variable b_i and premultiplying by q_k^T one obtains:

$$2\omega_k \frac{\partial \omega_k}{\partial b_i} q_k^T M q_k = q_k^T \left(\left(\frac{\partial K}{\partial b_i} - \omega_k^2 \frac{\partial M}{\partial b_i} \right) q_k + \left(K - \omega_k^2 M \right) \frac{\partial q_k}{\partial b_i} \right) \tag{61}$$

Considering the modal normalization $q_k^T M q_k = 1$, the sensitivity of the natural frequency corresponding to mode k with respect to changes in design variables is given by:

$$\frac{\partial \omega_k}{\partial b_i} = \frac{1}{2\omega_k} q_k^T \left(\frac{\partial K}{\partial b_i} - \omega_k^2 \frac{\partial M}{\partial b_i} \right) q_k \tag{62}$$

where $\partial M / \partial b_i$ is the system mass sensitivity matrix. Thus, in order to evaluate the sensitivity of natural frequencies with respect to changes in the design variables there is no need to define an adjoint structure.

4. Sensitivity analysis of axisymmetric shells

The analytical derivative of the element stiffness matrix (eqs. 37 and 38) with respect to a variable b_k^* (not necessarily a design variable) can be represented in a symbolic form as:

$$\frac{\partial K_n^e}{\partial b_k^*} = \int_0^{2\pi} \int_0^1 \left\{ \left[\left(B^T D \frac{\partial B}{\partial b_k^*} \right)^T + \left(B^T D \frac{\partial B}{\partial b_k^*} \right) + \left(B^T \frac{\partial D}{\partial b_k^*} B \right) \right] \ell r + \right.$$
$$\left. + (B^T D B) \left(\ell \frac{\partial r}{\partial b_k^*} + r \frac{\partial \ell}{\partial b_k^*} \right) \right\} d\zeta d\theta \tag{63}$$

where:

$$D = \begin{bmatrix} D_m & 0 \\ 0 & D_f \end{bmatrix}; \quad B = \begin{bmatrix} B_{m_n} \\ B_{f_n} \end{bmatrix}$$

The derivative of the element force vector is:

$$\frac{\partial p_n^e}{\partial b_k^*} = \int_0^{2\pi}\int_0^1 \left\{\left[\left(\frac{\partial L^T}{\partial b_k^*} N_n^T f_n^e\right) + \left(L^T \frac{\partial N_n^T}{\partial b_k^*} f_n^e\right) + \left(L^T N_n^T \frac{\partial f_n^e}{\partial b_k^*}\right)\right] \ell r + \right.$$
$$\left. + \left(L^T N_n^T f_n^e\right)\left(\frac{\partial r}{\partial b_k^*}\ell + r\frac{\partial \ell}{\partial b_k^*}\right)\right\} d\xi d\theta \tag{64}$$

The derivatives of the mass matrix are obtained in a similar way.

The derivatives of the arguments are evaluated at each Gauss point, separately for membrane and bending, and numerical integration is used. Alternatively, when the design variables are radial coordinates, the derivatives of Eq. (63) and mass matrix, and the integration of Eq. (64) and their derivatives $\partial p_n^e/\partial b_k^*$ is carried out using a symbolic manipulator. Full details are presented in Barbosa (1990).

When the design variables are thicknesses the sensitivities of stiffness matrix K^e or mass matrix M^e, are easily obtained. In fact the mass matrix M^e depends explicitly on the thickness while for the stiffness matrix K^e the dependence is only in constitutive matrices D_m and D_f. Assuming the thickness constant within the element one obtains:

$$\frac{\partial K_n^e}{\partial h} = \frac{1}{h}K_{m_n}^e + \frac{3}{h}K_{f_n}^e \tag{65}$$

$$\frac{\partial M_n^e}{\partial h} = \frac{1}{h}M_{n_T}^e + \frac{3}{h}M_{n_R}^e \tag{66}$$

where, respectively, $K_{m_n}^e$, $K_{f_n}^e$, $M_{n_T}^e$ and $M_{n_R}^e$ are the membrane and bending terms of the element stiffness matrix and the terms of element mass matrix due to translational and rotational inertia.

For nodal coordinates or when the thickness distribution varies within the element, the shape of the model is related through the linking relation (Vanderplaats, 1984):

$$l = l^c + Tb \tag{67}$$

where l is the vector of dependent variables (thicknesses and/or radial nodal coordinates of the finite element model), T the linking matrix which relates the vector of shape design variables b with the dependent variables and l^c a vector of constant terms.

With regard to shape design variables and considering the linking relation (Eq. 67), the sensitivities of the element stiffness, mass or load vector can also be obtained analytically through:

$$\frac{\partial F^e}{\partial b_i} = \sum_{k=1}^{2} \frac{\partial F^e}{\partial b_k^*}\frac{\partial b_k^*}{\partial b_i} = \sum_{k=1}^{2} \frac{\partial F^e}{\partial b_k^*} T_{ki}^e \quad i = 1, n \tag{68}$$

where F^e can be the stiffness and mass matrices or load vector of the eth element and T_{ki}^e is related to the linking matrix T through the topological finite element

code procedure, b_k^* being the value of the element nodal variable concerned, namely, the nodal coordinates of the two ring node frustum conical element $(r_k^e, z_k^e;\ k = 1, 2)$.

For static constraints, the sensitivities are evaluated through the technique of adjoint structure assuming that the structure satisfies the equilibrium equation:

$$K_n \lambda_{j_n} = z_{j_n}. \tag{69}$$

For harmonic n, $z_{j_n} = \partial g_{j_n}/\partial q_n$ is the vector of adjoint forces, q_n the vector of system degrees of freedom and λ_{j_n} the system adjoint degrees of freedom for the constraint g_{j_n}.

The sensitivities of a constraint function or the sensitivity of natural frequency with respect to a design variable are evaluated efficiently at element level using equations:

$$\frac{dg_j}{db_i} = \sum_{n=0}^{N} \left(\frac{\partial g_{j_n}}{\partial b_i} + \sum_{e \in E} \lambda_{j_n}^{e^T} \left(\frac{\partial p_n^e}{\partial b_i} - \frac{\partial K_n^e}{\partial b_i} q_n^e \right) \right) \tag{70}$$

$$\frac{d\omega_k}{db_i} = \frac{1}{2\omega_{k_n}} \sum_{e \in E} q_{j_n}^{e^T} \left(\frac{\partial K_n^e}{\partial b_i} - \omega_{k_n}^2 \frac{\partial M_n^e}{\partial b_i} \right) q_{k_n}^e \tag{71}$$

E being the set of elements e which are affected by the design variable b_i and N the total number of harmonic terms. The element vectors λ_j^e, q^e and q_k^e are related with the system vectors λ_j, q and q_k of the nth harmonic, through the topological finite element code procedure.

Semi–analytical method

In this technique the vector of adjoint forces is obtained analytically and the gradients of equations (58) and (62), with terms of the type $\partial F/\partial b_i$, are evaluated by forward finite difference (FFD) technique through the approximation:

$$\frac{\partial F}{\partial b_i} \approx \frac{F(b + \Delta b) - F(b)}{\delta b_i} \tag{72}$$

where $\Delta b = [0, \ldots, \delta b_i, \ldots, 0]$ and δb_i is a small perturbation. It should be noticed that to evaluate $F(b + \Delta b)$ for shape optimization, it is required to calculate the coordinate perturbations δr due to a design perturbation δb_i and these are carried out through the linking relation.

Finite difference technique

A global finite difference approach is also used through forward finite difference and, alternatively, central finite difference (CFD). The sensitivities of a constraint with respect to a change δb_i in a design are then evaluated as:

$$\frac{dg_j}{db_i} \approx \frac{g_j(b + \Delta b) - g_j(b)}{\delta b_i} \qquad \text{(FFD)} \tag{73}$$

$$\frac{dg_j}{db_i} \approx \frac{g_j(b+\Delta b) - g_j(b-\Delta b)}{2\delta b_i} \quad \text{(CFD)} \tag{74}$$

which needs, respectively, one or two extra structural analyses for each design variable.

5. Constraints

Limit on displacements

A constraint on a displacement is represented in a normalized form by:

$$g_j = \frac{q_f}{q_0} - 1 \leq 0 \tag{75}$$

where q_f is the real generalized displacement corresponding to system degree of freedom f and q_0 is the maximum admissible generalized displacement.

Expanding q_f by Fourier series, one obtains the vector of adjoint forces for the nth harmonic as:

$$z_{j_n} = \left[\frac{\partial g_{j_n}}{\partial q_1} \cdots \frac{\partial g_{j_n}}{\partial q_f} \cdots \frac{\partial g_{j_n}}{\partial q_p}\right]^T = \left[0 \cdots \frac{C_s}{q_0} \cdots 0\right]^T \tag{76}$$

where p is the total number of degrees of freedom and $C_s = \cos n\theta$ or $C_s = \sin n\theta$ relating the corresponding degree of freedom. For a general arbitrary loading, these vectors are obtained easily for the anti–symmetric terms. It should be noticed that the adjoint structure is identical to the real structure and it is subjected to a force or moment of intensity C_s/q_0 on the corresponding degree of freedom where the displacement or rotation is limited.

Thus the sensitivity of a displacement constraint evaluated by Eq. (70), yields:

$$\frac{dg_j}{db_i} = \sum_{n=0}^{N} \sum_{e \in E} \lambda_{j_n}^{e^T} \left(\frac{\partial p_n^e}{\partial b_i} - \frac{\partial K_n^e}{\partial b_i} q_n^e\right) \tag{77}$$

For arbitrary loading, the final value of the sensitivity is then obtained by adding the corresponding contribution of the symmetric and anti–symmetric terms.

Limit on stresses

Limit on a stress or an effective stress is represented by:

$$g_j = \frac{\overline{\sigma}}{\sigma_0} - 1 \leq 0 \tag{78}$$

where σ_0 is the maximum allowable stress, which may be different for tension and compression, and $\overline{\sigma}$ is the stress component or the effective stress which

one pretends to constraint. For this particular element, the stresses, for the nth harmonic, are evaluated as:

$$\sigma_n^m = \frac{1}{h} D_m B_{m_n} q_n^e = A_n q_n^e \quad \text{(membrane stresses)} \tag{79}$$

$$\sigma_n^f = \frac{6}{h^2} D_f B_{f_n} q_n^e = G_n q_n^e \quad \text{(bending stresses)} \tag{80}$$

where:

$$\sigma_n^m = [\sigma_{SS_n}^m \;\; \sigma_{\theta\theta_n}^m \;\; \sigma_{S\theta_n}^m]^T; \qquad \sigma_n^f = [\sigma_{SS_n}^f \;\; \sigma_{\theta\theta_n}^f \;\; \sigma_{S\theta_n}^f]^T \tag{81}$$

$$A_n = [A_{n_1} \;\; A_{n_2} \;\; A_{n_3}]^T; \qquad G_n = [G_{n_1} \;\; G_{n_2} \;\; G_{n_3}]^T \tag{82}$$

with $(\sigma_{SS_n}^m;\ \sigma_{SS_n}^f)$ and $(\sigma_{\theta\theta_n}^m;\ \sigma_{\theta\theta_n}^f)$ being the meridional and circumferential components of normal stresses and $(\sigma_{S\theta_n}^m,\ \sigma_{S\theta_n}^f)$ the shear stress components for membrane and bending, respectively, for the nth harmonic.

In the case of a meridional stress at the extreme fibers, the stress component is represented as:

$$\overline{\sigma} = \sigma_{SS_n}^m \pm \sigma_{SS_n}^f \tag{83}$$

For example, a stress constraint at Gauss point of element c corresponds to the element adjoint load vector $z_{j_n}^c$ given by:

$$z_{j_n}^c = \frac{\cos n\theta}{\sigma_0} \left(A_{n_1}^T \pm G_{n_1}^T\right) \tag{84}$$

The system adjoint force vector z_{j_n}, for the nth harmonic, is assembled in a similar way as the system load vector (Eq. 50)

Thus, for a pointwise limit on a stress, such as defined by Eq. (78), the sensitivity of stress constraint to thickness variation, evaluated by Eq. (70), yields:

$$\frac{dg_j}{dh_i} = \sum_{n=0}^{N} \left[\frac{\sigma_{SS_n}^f}{\sigma_0 h} - \sum_{e \in E} \lambda_{j_n}^{e^T} \frac{\partial K_n^e}{\partial h_i} q_n^e \right] \tag{85}$$

h being the thickness of the cth element where the constraint g_j has been imposed. If the design variable is a radial coordinate, then Eq. (70) can be represented as:

$$\frac{dg_j}{dh_i} = \frac{1}{\sigma_0} \sum_{n=0}^{N} \left(\sum_{k=1}^{2} \frac{\partial}{\partial r_k^c} (A_{n_1} \pm G_{n_1}) T_{ki}^c q_n^c - \sum_{e \in E} \lambda_{j_n}^{e^T} \left(\frac{\partial p_n^e}{\partial b_i} - \frac{\partial K_n^e}{\partial b_i} q_n^e \right) \right) \tag{86}$$

where the first terms of the second member of Eqs. (85) and (86) are evaluated only for the cth element where the stress constraint is imposed.

In the semi–analytical method, one obtains for the explicit term of Eq. (70) and only for the element with stress constraint :

$$\frac{\partial g_j}{\partial b_i} \approx \frac{1}{\sigma_0 \delta b_i} \{[A_{n_1}(r_1^c + \delta r_1^c, z_1^c;\ r_2^c + \delta r_2^c, z_2^c) - A_{n_1}(r_1^c, z_1^c;\ r_2^c, z_2^c)] \pm [G_{n_1}(r_1^c + \delta r_1^c, z_1^c;\ r_2^c + \delta r_2^c, z_2^c) - G_{n_1}(r_1^c, z_1^c;\ r_2^c, z_2^c)]\}\, q_n^c \tag{87}$$

Limit on natural frequencies

A constraint in the natural frequency of mode k can be easily evaluated once the eigenvalue problem is solved. Consider a normalized constraint of the type:

$$g_j = 1 - \frac{\omega_k}{\omega_0} \leq 0 \tag{88}$$

The sensitivity given by Eq. (71) is evaluated as:

$$\frac{dg_j}{db_i} = -\frac{1}{2\omega_0 \omega_k} \sum_{e \in E} q_{k_n}^{e^T} \left(\frac{\partial K_n^e}{\partial b_i} - \omega_{k_n}^2 \frac{\partial M_n^e}{\partial b_i} \right) q_{k_n}^e \tag{89}$$

where ω_0 is the limiting natural frequency for mode k.

Limit on volume of the shell material

For the present frustum–cone finite element, the volume of the shell material is given by:

$$V = \sum_{e=1}^{I} V^e = \pi \sum_{e=1}^{I} \sqrt{(r_2^e - r_1^e)^2 + (z_2^e - z_1^e)^2}\,(r_1^e + r_2^e) h^e \tag{90}$$

where I is the total number of elements.

Impose the initial volume V_0 of the shell material of the structure as constant and consider a normalized equality constraint of the type:

$$g_j = \frac{V}{V_0} - 1 = 0 \tag{91}$$

The derivatives are easily obtained for constant thickness and radial coordinates, yielding, respectively:

$$\frac{dg_j}{dh_i} = \frac{\pi}{V_0} \sum_{e \in E} \ell (r_1^e + r_2^e) \tag{92}$$

$$\frac{dg_j}{db_i} = \frac{\pi}{V_0} \sum_{e \in E} h^e \left\{ \left(-\frac{(r_2^e)^2 - (r_1^e)^2}{\ell} + \ell \right) T_{1i}^e + \left(\frac{(r_2^e)^2 - (r_1^e)^2}{\ell} + \ell \right) T_{2i}^e \right\} \tag{93}$$

Limit on enclosed volume of the structure

The enclosed volume of the structure is given by:

$$C = \sum_{e=1}^{J} C^e = \frac{\pi}{3} \sum_{e=1}^{J} \left((r_2^e)^2 + (r_1^e)^2 + (r_1^e r_2^e) \right) |(z_2^e - z_1^e)| \tag{94}$$

J being the total number of finite elements which are related to the enclosed volume.

Assume the initial enclosed volume C_0 of the structure as constant and consider a normalized equality constraint of the type:

$$g_j = 1 - \frac{C}{C_0} = 0 \tag{95}$$

Thus the sensitivity of constraint on the enclosed volume of the structure with respect to radial nodal coordinates perturbation yields:

$$\frac{dg_j}{db_i} = -\frac{\pi}{3C_0} \sum_{e \in E} (|(z_2^e - z_1^e)|) \{ (r_2^e + 2r_1^e) T_{1i}^e + (2r_2^e + r_1^e) T_{2i}^e \} \tag{96}$$

6. Optimal design

The objective is minimization of the volume V of the material, maximization of natural frequency ω_k, minimization of the maximum stress $\overline{\sigma}$ or minimization of the maximum displacement q_f. The problem is stated as:

$$\min V(b) \quad \text{or} \quad \max \omega_k(b) \quad \text{or} \quad \min(\max \overline{\sigma}(b)) \quad \text{or} \quad \min(\max q_f) \tag{97}$$

subject to:

$$\begin{array}{lll} g_j(b) \leq 0 & j = 1, i & \text{a)} \\ g_k(b) = 0 & k = i+1, m & \text{b)} \\ b_{\mathrm{i}}^d \leq b_{\mathrm{i}} \leq b_{\mathrm{i}}^u & \mathrm{i} = 1, 2, \ldots, n & \text{c)} \end{array} \tag{98}$$

Constraints g_j are inequality constraints (such as displacement or stress) and g_k are equality constraints (enclosed volume of the structure or the volume of the shell material), b_{i}^d and b_{i}^u are the lower and upper limiting bounds of the design variables and i, m, n are the number of inequality constraints, total number of constraints and total number of design variables, respectively.

Bound formulation, Taylor and Bendsøe (1984), is used to solve min–max problem. The problem is restated as a simple minimization problem in terms of a bound β on the value of max $\overline{\sigma}$:

$$\min \beta \tag{99}$$

with:

$$(\beta - \epsilon\beta) < \max \overline{\sigma} \leq \beta \tag{100}$$

where ϵ is defined by the user.

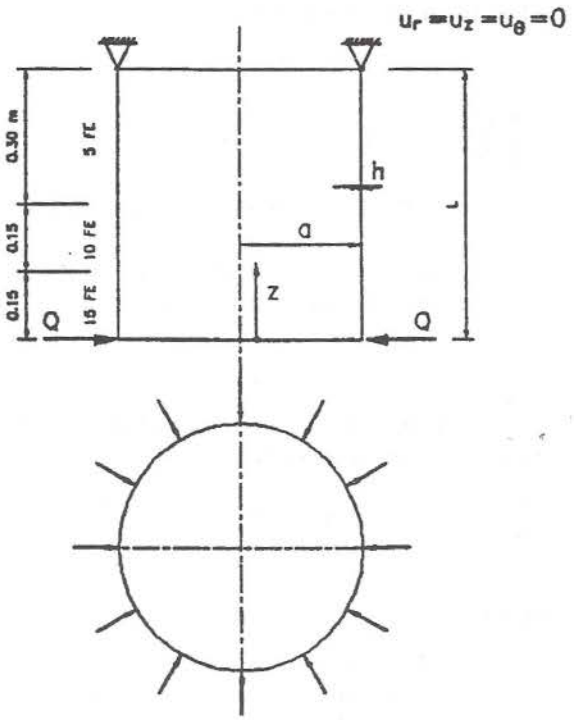

Figure 2. Cylinder. Geometry and load

7. Applications

A computer program for personal computers has been developed based on the formulation presented. The illustrative optimal designs shown in this paper where obtained using the modified feasible direction method of the ADS program, described by Vanderplaats (1984).

Supported cylinder with end shearing force

The load, geometric and material properties are: $Q = 1000\text{N/m}$; $a = 1\text{m}$; $h = 0.01\text{m}$; $L = 0.6\text{m}$; $E = 200$ GPa (Young's modulus); $\nu = 0.30$ (Poisson's coefficient). A finite element model with 30 elements was considered (Fig. 2). The design variable is the thickness of the cylinder.

The radial displacement distribution of the Love–Kirchhoff analytical solution (Kraus, 1967) is:

$$u_r = -\frac{Q}{2\mu^3 D} e^{-\mu z} \cos(\mu z); \quad \mu = \left(\frac{3(1-\nu^2)}{a^2 h^2}\right)^{1/4}; \quad D = \frac{Eh^3}{12(1-\nu^2)}$$

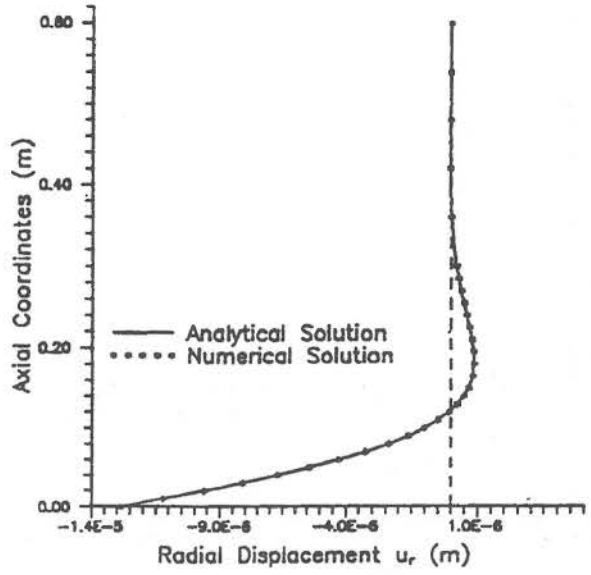

Figure 3. Radial displacements distribution.

which compares very favourably with the present numerical solution (Fig. 3).

The sensitivity distribution obtained using discrete finite element model with the analytical method has a very good agreement (Fig. 4) with the theoretic sensitivity obtained by differentiating the above expression using a symbolic manipulator, yielding:

$$\frac{du_r}{dh} = \frac{dg}{dh} = \frac{P_1 \cos(P_2)}{P_3 h^{(\frac{5}{2})} E} - \frac{P_4 \cos(P_2)}{P_3 h^3 E} - \frac{P_4 \sin(P_2)}{P_3 h^3 E}$$

where :

$$P_1 = 3.948 Q a^{\frac{3}{2}} (1-\nu^2)^{\frac{1}{4}}; \quad P_2 = \frac{1.316 z (1-\nu^2)^{\frac{1}{4}}}{(ah)^{\frac{1}{2}}}$$

$$P_3 = e^{\left(\frac{1.316 z (1-\nu^2)^{\frac{1}{4}}}{\sqrt{ah}}\right)}; \quad P_4 = 1.732 Q a z \sqrt{(1-\nu^2)}$$

Simply supported cone–cylinder connection with internal pressure

The geometric and material properties are: $R = 1.0$ m (cylinder radius), $H = 0.6$ m (height of cylinder), $h = 0.010$ m (thickness), $E = 200$GPa, $\nu = 0.3$.

A finite element model with 50 elements was considered (Fig. 5). The design variables are 6 radial coordinates $(b_1, \ldots, b_6)$. Tables 1 and 2 show the sensitivities for the initial design with respect to changes in the radial coordinates

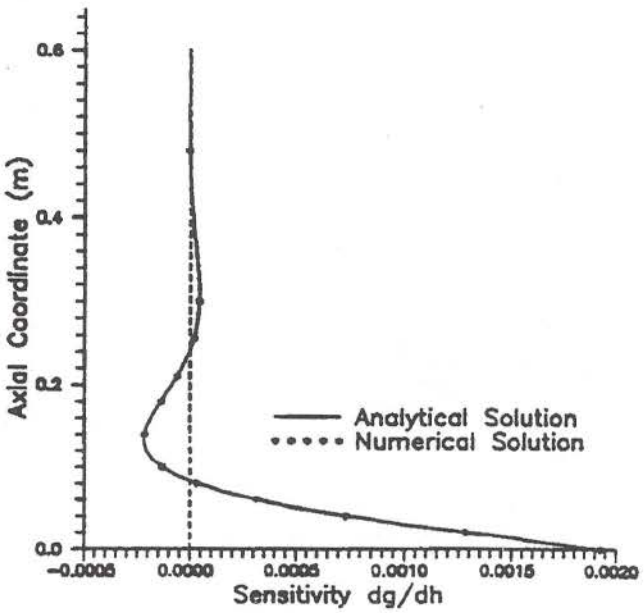

Figure 4. Sensitivity distribution.

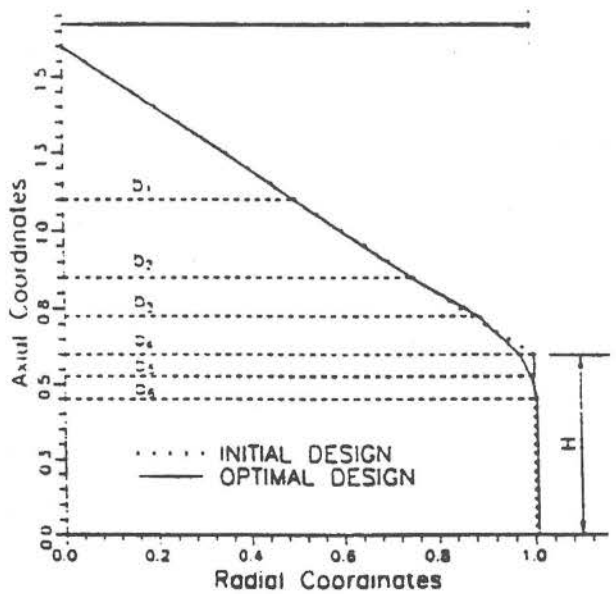

Figure 5. Minimization of maximum stress

Source	Perturbation	Sensitivities					
		b_1	b_2	b_3	b_4	b_4	b_6
CFD	$0.001b_i$	-0.0430	0.6042	4.6708	-12.7946	0.0926	5.7383
Analytical		-0.0430	0.6041	4.6703	-12.7940	0.0922	5.7387
Semi–Analytical	$0.000000001b_i$	-0.0430	0.6042	4.6708	-12.7946	0.0922	5.7387
	$0.0000001b_i$	-0.0430	0.6042	4.6709	-12.7942	0.0928	5.7390
	$0.00001b_i$	-0.0430	0.6044	4.6811	-12.7507	0.1541	5.7679
	$0.001b_i$	-0.0428	0.6289	5.7062	-8.4132	6.2830	8.6519
	$0.01b_i$	-0.0410	0.8691	15.9369	29.7409	61.1342	34.3096

Table 1. Sensitivities due to a radial displacement constraint

Source	Perturbation	Sensitivities					
		b_1	b_2	b_3	b_4	b_4	b_6
CFD	$0.001b_i$	-0.0077	0.8343	-6.5946	16.7119	-7.8595	-1.8374
Analytical		-0.0077	0.8342	-6.5940	16.7115	-7.8591	-1.8375
Semi–Analytical	$0.000000001b_i$	-0.0077	0.8343	-6.5946	16.7121	-7.8591	-1.8375
	$0.0000001b_i$	-0.0077	0.8343	-6.5947	16.7114	-7.8598	-1.8376
	$0.00001b_i$	-0.0077	0.8344	-6.6034	16.6458	-7.9269	-1.8488
	$0.001b_i$	-0.0077	0.8480	-7.4871	10.0850	-14.6369	-2.9660
	$0.01b_i$	-0.0077	0.9802	-16.3546	-48.1310	-74.5055	-12.912

Table 2. Sensitivities due to a meridional stress constraint

for a displacement radial constraint in the junction ($r = 1.0$ m, $z = 0.6$ m) and a meridional stress constraint σ_{SS} in the Gaussian point of the cylindrical element adjacent to the junction. The cone-cylinder connection is submitted to an internal pressure of $p = 0.2$MPa. The global sensitivities are calculated using central finite difference (CFD) with a perturbation of $\Delta b_i = 0.001 b_i$.

From Tables 1 and 2 it is observed that the analytical sensitivities for shape design sensitivities compare very favourably with the global finite element sensitivities obtained with the same model. It is also seen that the semi–analytical sensitivities only compare favourably for very small perturbations in the design variables, being highly influenced by the perturbation used, due to the truncation on the finite difference method.

For the initial design the maximum meridional stress is $\sigma_{SS} = 105.4$ MPa at the cylindrical element adjacent to the junction. The model is optimized considering a radial deflection of $u_{r_0} = 0.3$ mm, a meridional stress limit of $\sigma_0 = 120$ MPa and the enclosed volume of the initial design at 2.932 m^3 (equality constraint).

The optimal design is obtained in 14 iterations, 34 function evaluations and 6 gradient evaluations, with a reduction of maximum stress of 68%. During the

	AM / SA	FFD / SA	CFD / SA
CPU ratio	2.5	3.2	5.4

Table 3. Evaluation of sensitivities

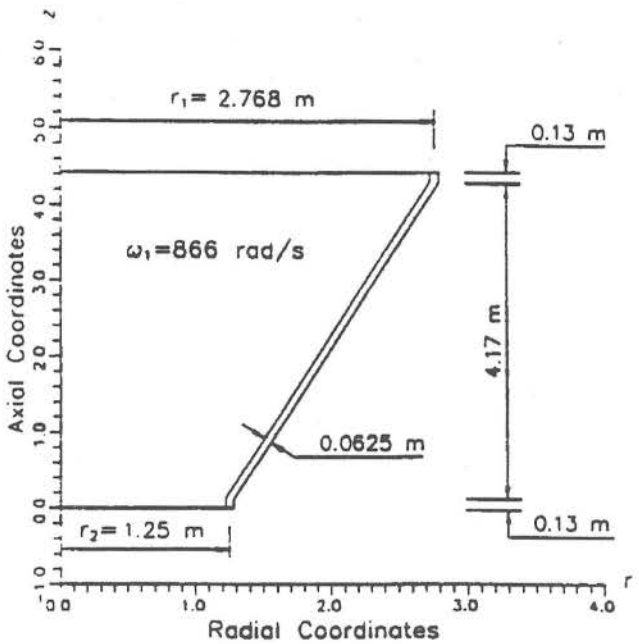

Figure 6. Initial design

iteration process the enclosed volume of the initial design is an active constraint. For the optimal design the maximum meridional stress in the model decreases to $\sigma_{SS} = 33.5$ MPa.

A CPU ratio of 2.5 is achieved between the analytical/semi–analytical evaluation of sensitivities. Table 3 shows the CPU ratio between semi–analytical method (SA) versus analytical method (AM), global central finite difference (CFD) and global forward finite difference (FFD).

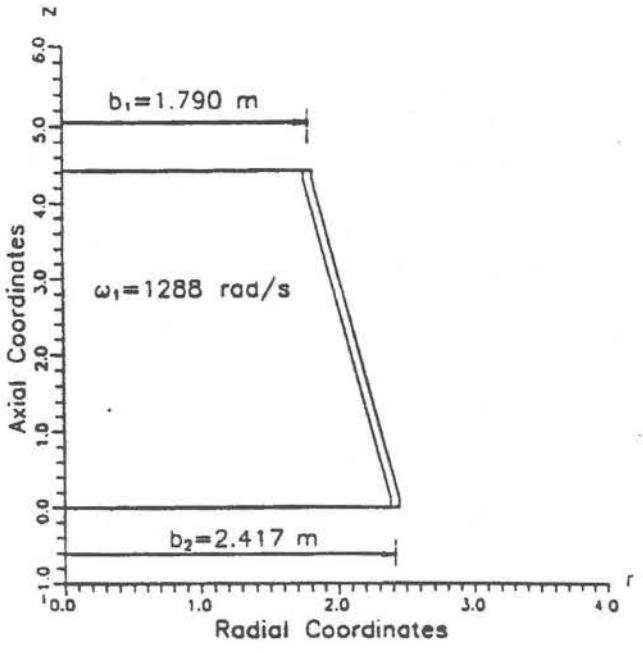

Figure 7. Optimal design (1st level)

Conical structure clamped at lower end

A conical shell clamped at lower end with geometry shown in Fig. 6 and material properties $E = 200$ GPa (Young's modulus), $\nu = 0.15$ (Poisson's coefficient) and $\varrho = 2410$ Kg·m^{-3} (mass per unit volume) is considered. The structure has been modelled with 68 elements.

Table 4 shows the sensitivity results for the initial design with a good agreement between the three methods.

A two level optimization has been carried out. The objective of the design is the maximization of the fundamental frequency for the harmonic $n = 0$, with a constraint of enclosed volume of the structure in the first level and a constraint of volume of the shell material in the second level.

On the first level the design variables are 2 radial coordinates b_1 and b_2. The optimal design (Fig.7) is obtained in 8 iterations, 41 function evaluations and 7 gradient evaluation, with an increase in natural frequency of 49%. During the iteration process the active constraint is the enclosed volume of the structure (equality constraint) that is imposed constant and equal to 59.157 m^3. The natural frequency of the optimum solution is in agreement with the plot (Fig.8) of natural frequency versus radial coordinates carried out through 12 finite element analyses using constant enclosed volume (59.157 m^3) for the structure.

On the 2nd level of optimization the design variables are 6 thicknesses, where

Source	Perturbation	Sensitivities	
		b_1	b_2
FFD	$0.001b_i$	-271.606	284.140
Analytical		-271.637	284.192
Semi–Analytical	$0.000000001b_i$	-271.720	284.192
	$0.0000001b_i$	-271.724	284.182
	$0.00001b_i$	-271.725	284.183
	$0.001b_i$	-272.109	285.353
	$0.01b_i$	-273.633	290.049

Table 4. Sensitivities due to fundamental frequency

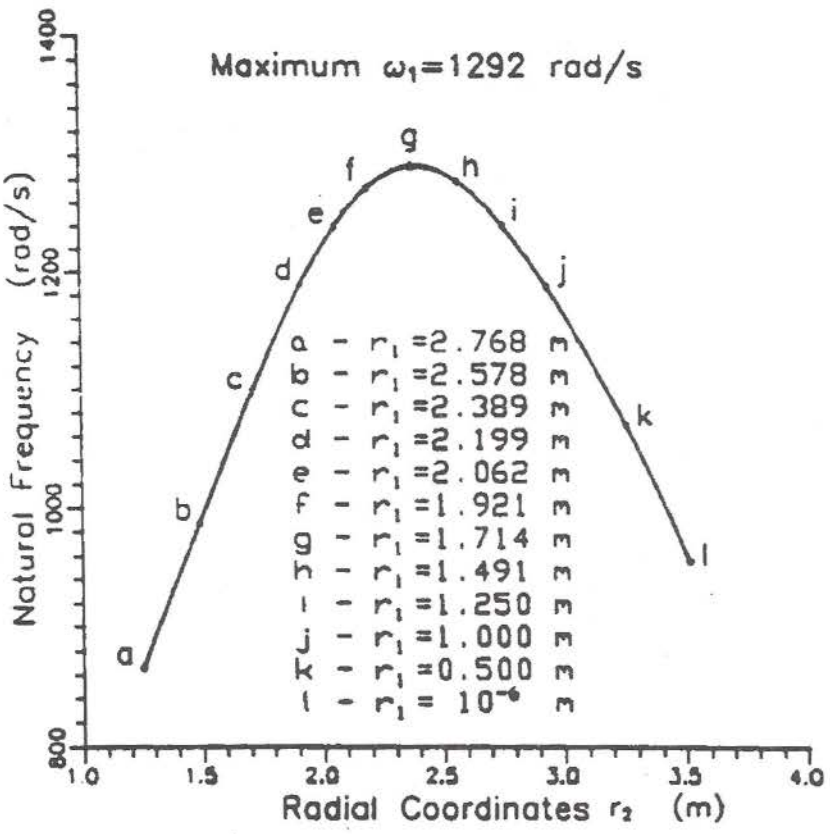

Figure 8. FEM analysis

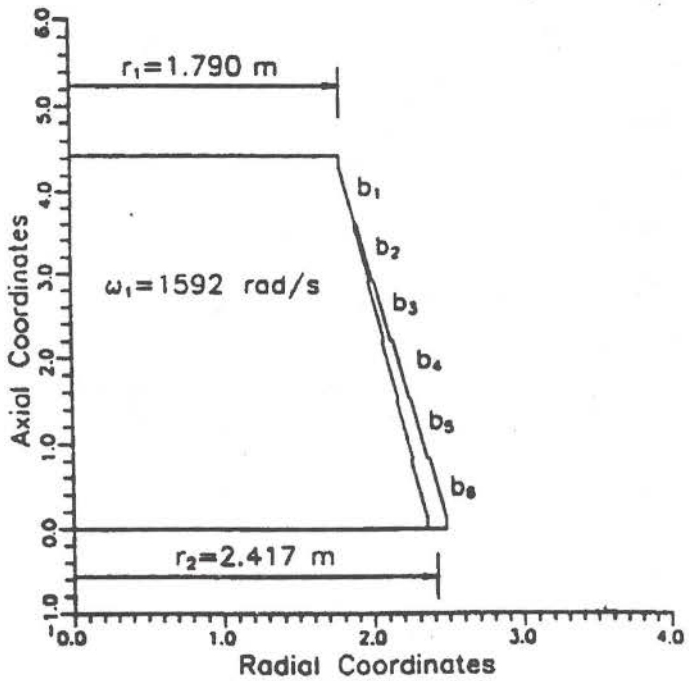

Figure 9. Optimal design (2st level)

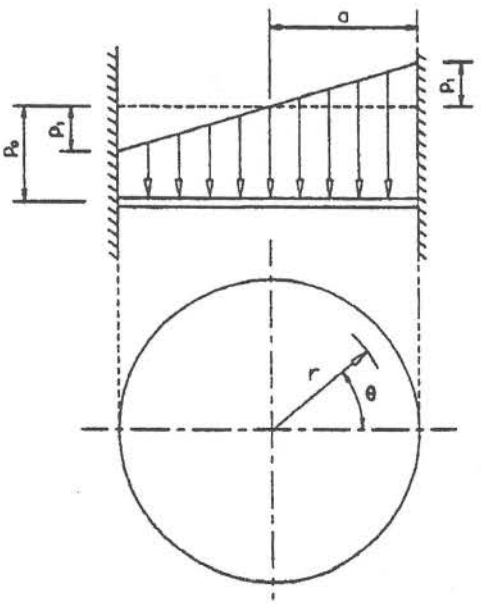

Figure 10. Clamped circular plate. Geometry and load.

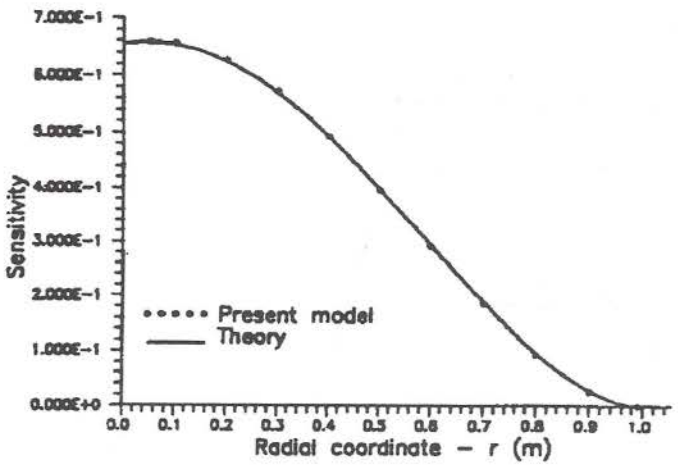

Figure 11. Sensitivities. Displacement constraint

the initial design is the final design of the first level of optimization. The constraint is the volume of the shell material that is imposed constant and equal to 3.706 m^3. The optimal design (Fig.9) is obtained in 7 iterations, 27 function evaluations and 5 gradient evaluation, with a further increase in natural frequency of 24%.

Clamped circular plate

The material and geometric properties (Fig. 10) are $E = 200$ GPa, $\nu = 0.30$, $a = 1$ m, $h = 0.025$ m and the load is given by $p = p_0 + p_1 \frac{r}{a} \cos\theta$; $p_0 = 100\,000$ Pa; $p = 50\,000$ Pa.

The plate has been modelled with 20 finite elements. Fig. 11 and Fig. 12 show the sensitivity distribution due to thickness variation and constraints of displacement in $r = 0$ and stress $\overline{\sigma}$ at $r = 0.97$ m. They are compared with the results obtained using the theoretic sensitivity obtained by differentiating the expressions of Love–Kirchhoff shell theory. The agreement between the proposed model and the alternative results is quite favourable.

The objective of the design is the minimization of the volume of the circular plate that has been optimized considering deflection and stress limits of $q_0 = 9$ mm and $\sigma_0 = 150$ MPa, respectively. The upper limiting bound of the design variables has been set to $h \leq 50$ mm.

The optimal design when five design variables (thicknesses) are considered is shown in Fig. 13 and is obtained with 9 iterations, 33 functions evaluations and 5 gradient evaluations. The reduction in volume with regard to the initial design was 21.2%. Both constraints are activated and the stresses are calculated for $\theta = 0°$; $\theta = 45°$; $\theta = 90°$; $\theta = 135°$; $\theta = 180°$; $\theta = 225°$; $\theta = 270°$ and $\theta = 315°$.

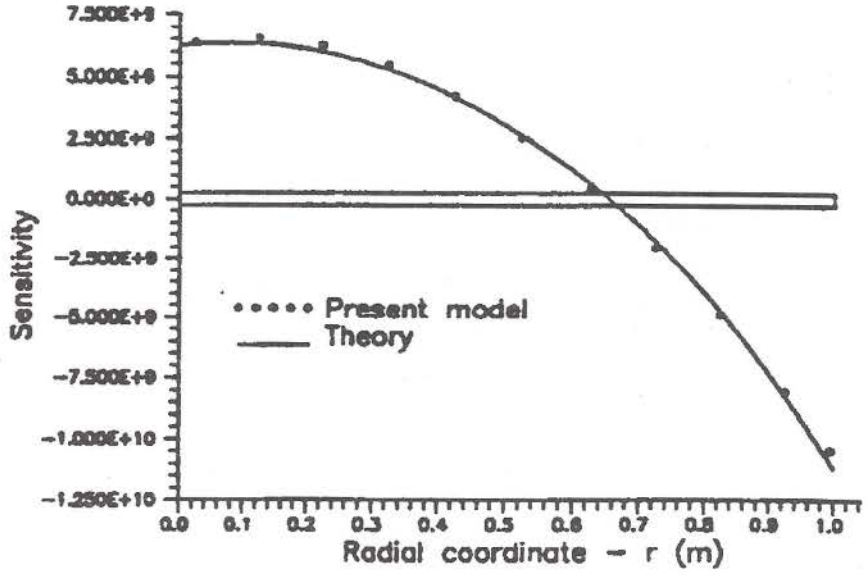

Figure 12. Sensitivities. Stress constraint

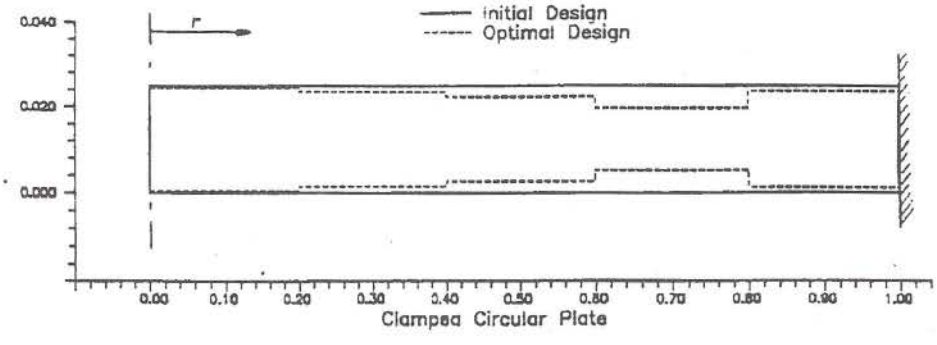

Figure 13. Clamped circular plate — optimal design

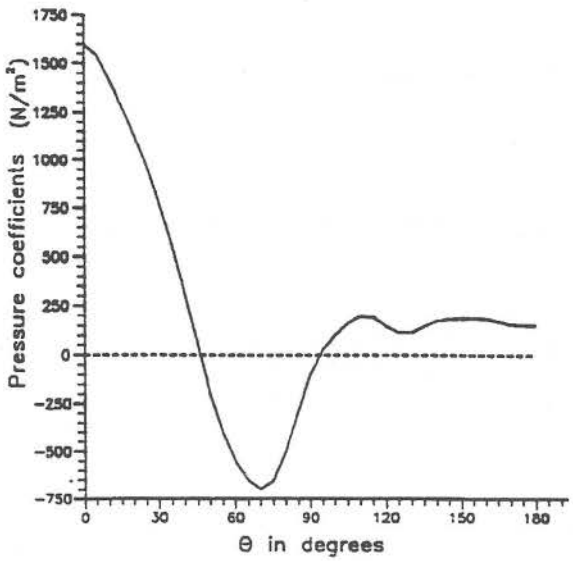

Figure 14. Surface load variation

Double supported cylinder–cone–cylinder connection

The geometry for the initial design (Fig. 15) and material properties are: $b_1 = b_2 = 0.8$ m; $b_3 = 1.1$ m; $b_4 = b_5 = 1.4$ m; $h = 0.012$ m; $H = 2.2$ m (Height of connection); $E = 200$ GPa; $\nu = 0.3$.

A finite element model with 50 elements has been considered. The design variables are 5 radial coordinates $(b_1, \ldots, b_5)$. Tables 5 and 6 show the sensitivities for the initial design with respect to changes in the radial coordinates for a maximum displacement radial constraint and for meridional stress using bound formulation. The cylinder–cone–cylinder connection is submitted to a external surface load with the distribution represented in Fig. 14.

From Tables 5 and 6 it is observed that the analytical sensitivities for shape design compare very favourably with the global finite element sensitivities obtained with the same model. As in axisymmetric loading, it is also seen that the semi–analytical sensitivities only compare favourably in some design variables for very small perturbations, being highly influenced by the perturbation used, due to the truncation on the finite difference method. The results obtained for b_5 using bound formulation are in discrepancy for all the perturbations used.

A CPU ratio of 2.1 is achieved between the analytical/semi-analytical evaluation of sensitivities for a radial displacement constraint and a ratio of 1.9 for bound formulation.

The double supported cylinder–cone–cylinder connection has been first optimized considering deflection and stress limits of, respectively, $q_0 = 1$ mm and $\sigma_0 = 120$ MPa. The optimal design is shown in Fig. 15 and is obtained with 35

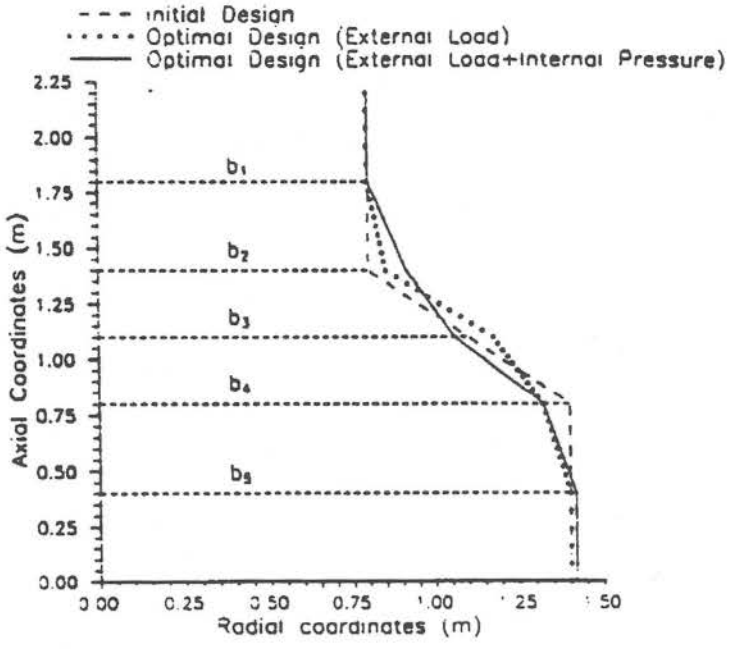

Figure 15. Cylinder–cone–cylinder connection

Source	Perturbation	Sensitivities $\times 10^{-2}$				
		b_1	b_2	b_3	b_4	b_5
Analytical		-0.06193	-0.9331	1.722	-0.7951	-0.3052
CFD	$0.001b_i$	-0.06194	-0.9331	1.722	-0.7951	-0.3052
FFD	$0.001b_i$	-0.06213	-0.9331	1.723	-0.7946	-0.3052
Semi–Analytical	$0.000000001b_i$	-0.06205	-0.9329	1.722	-0.7953	-0.3051
	$0.0000001b_i$	-0.06204	-0.9329	1.722	-0.7952	-0.3051
	$0.00001b_i$	-0.06191	-0.9323	1.723	-0.7947	-0.3051
	$0.001b_i$	-0.04853	-0.8755	1.821	-0.7441	-0.3073
	$0.01b_i$	0.0730	-0.3451	2.712	-0.3091	-0.3269
	$0.03b_i$	0.342	0.923	4.692	0.511	-0.3686

Table 5. Sensitivities due to a radial displacement constraint

Source	Perturbation	Sensitivities $\times 10^{-2}$				
		b_1	b_2	b_3	b_4	b_5
Analytical		0.6249	-0.3942	-1.981	1.741	0.01773
CFD	$0.001b_i$	0.6263	-0.3894	-1.989	1.742	0.01759
FFD	$0.001b_i$	0.6259	-0.3898	-1.988	1.743	0.01756
Semi-Analytical	$0.000000001b_i$	0.5951	-0.3209	-2.023	1.954	-0.1016
	$0.0000001b_i$	0.5951	-0.3209	-2.023	1.954	-0.1016
	$0.00001b_i$	0.5947	-0.3219	-2.024	1.953	-0.1018
	$0.001b_i$	0.5478	-0.4290	-2.150	1.872	-0.1229
	$0.01b_i$	0.1211	-0.1426	-3.281	1.163	-0.3139
	$0.03b_i$	-0.825	-0.3800	-5.752	-0.249	-0.7303

Table 6. Sensitivities due to a meridional stress using bound formulation

iterations, 89 functions evaluations and 19 gradient evaluations. It was found a reduction in meridional stress, with regard to the initial design, of 39%. The maximum meridional stress in the model decreases from 0.638 MPa to 0.388 MPa. Only the enclosed volume of the initial design (8.872 m^3), equality constraint, is activated. The model has been also optimized considering the surface load distribution (Fig. 14) and an internal pressure of 0.5 MPa. The optimal design (Fig. 15) is obtained with 8 iterations, 19 functions evaluations and 3 gradient evaluations. In this case the maximum meridional stress in the model decreases from 117 MPa to 79 MPa. It was used for bound formulation $\epsilon = 0.2$ for the first 10 evaluations, $\epsilon = 0.1$ for the next 20 evaluations and $\epsilon = 0.05$ until the final design.

Pressure vessel

The last applications presented are pressure vessels with the same material properties ($E = 210$ GPa ; $\nu = 0.3$; $\varrho = 7800$ Kg·m^{-3}) and different geometries. The initial design (Fig. 16) has $r_1 = 0.8$ m, $r_2 = 1.4$ m, $h = 12$ mm and height $H = 19.5$ m. The structure has been modelled with 95 elements. The design variables are 7 thicknesses ($h_1 \ldots h_7$) and 1 radial coordinate b_1. Table 8 shows for the initial design the sensitivities due to fundamental frequency. For FFD a perturbation of $0.001b_i$ was used.

The objective of the design is to maximize of lower fundamental frequency. The analysis used 5 harmonic terms of Fourier series and 4 modes for each harmonic term. The optimal design was obtained in 5 iterations, 49 function evaluations and 5 gradient evaluations. During the iteration process the volume of the shell material of the initial design (1.656 m^3) was an active constraint and for thicknesses the interval 5 mm$\leq h_i \leq$ 50 mm for lower and upper bounds, respectively, was used. The lower fundamental frequency is given for the first mode of harmonic term $n = 1$ and it is increased from 36 rad/s in the initial

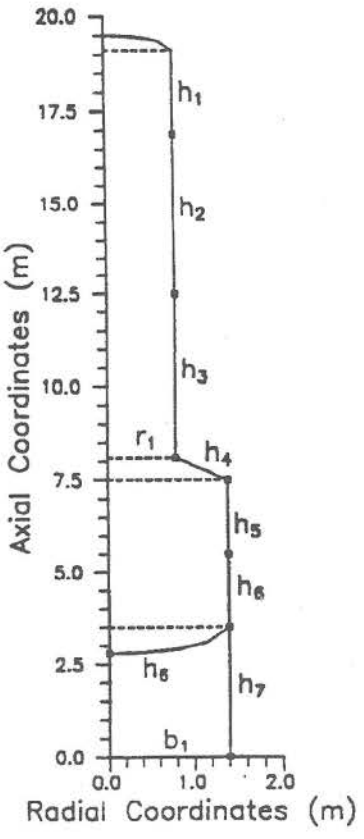

Figure 16. Initial design.

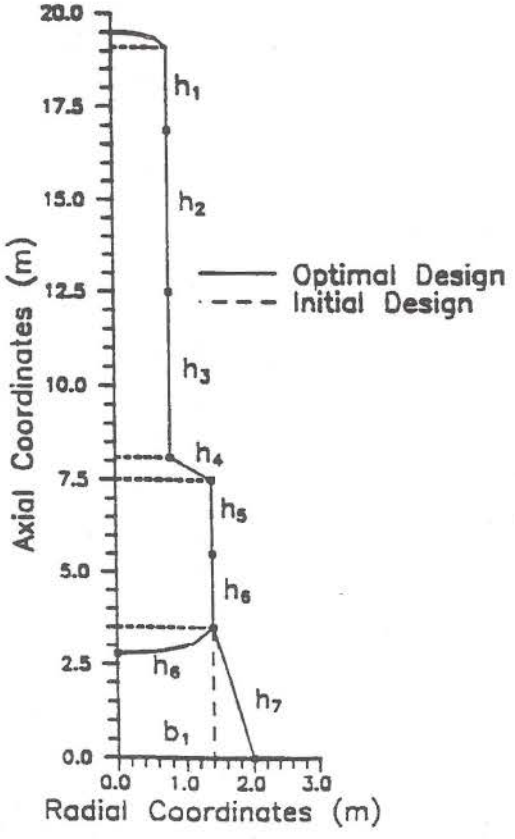

Figure 17. Minimization of maximum displacement.

Source	Sensitivities							
	h_1	h_2	h_3	h_4	h_5	h_6	h_7	b_1
Analytical	-809.3	-533.2	369.8	629.9	212.2	99.39	275.0	4.373
FFD	-809.0	-533.3	369.3	629.4	212.0	99.29	274.8	4.373

Table 7. Sensitivities due to fundamental frequency

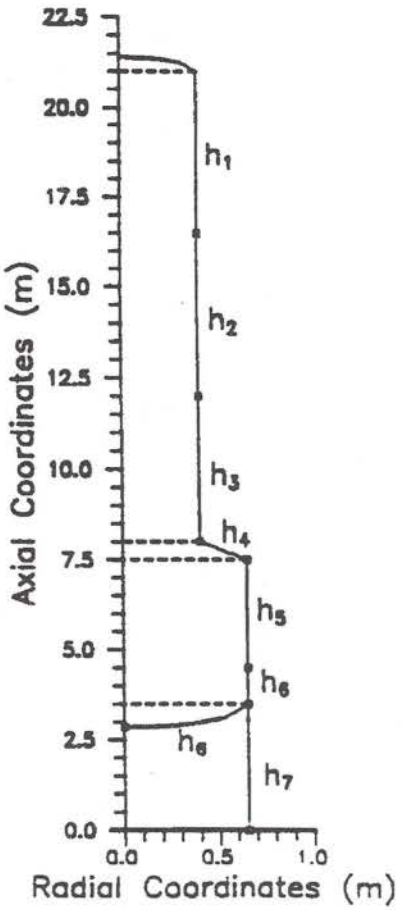

Figure 18. Initial design.

	Design variables (mm)							
Source	h_1	h_2	h_3	h_4	h_5	h_6	h_7	b_1
Initial	12.0	12.0	12.0	12.0	12.0	12.0	12.0	1400.
Optimal	5.00	5.00	12.3	48.4	11.2	9.54	15.7	1402.

Table 8. Design variables for initial and optimal designs

	Design variables (mm)						
	h_1	h_2	h_3	h_4	h_5	h_6	h_7
Mota Soares et al	22.6	22.8	22.9	40.4	34.6	34.7	4.7
Present	21.0	22.4	24.5	43.0	32.3	32.5	4.0

Table 9. Design variables for optimal design

design to 63 rad/s in the optimal design. Table 8 shows the design variables for optimal design.

The same geometry with thickness equal to 8 mm and same design variables was used to minimize the maximum displacement in node 1 ($r = 0; z = 19.5$). As lower and upper bounds 5 mm $\leq h_i \leq$ 12 mm and 0.15 m $\leq r_1 \leq$ 2 m were used. The pressure vessel was submitted to wind load (Fig. 14) and the displacements are calculated about circumference for $\theta = 0°$; $\theta = 45°$; $\theta = 60°$; $\theta = 90°$; $\theta = 135°$ and $\theta = 180°$. The optimal design (Fig. 17) was achieved in 2 iterations, 25 function evaluations and 2 gradient evaluations. The design variables (7 thicknesses and 1 radial coordinate) are set to the upper bounds in the final design and the reduction on displacement was 8.3% (2.743 mm to 2.516 mm)

The last case shown is a pressure vessel with the same material properties but using different geometry with $r_1 = 0.4$ m, $r_2 = 0.65$ m, $h_1 = h_2 = h_3 = 35$ mm, $h_4 = 45$mm, $h_5 = h_6 = h_7 = 40$ mm and height $H = 21.4$ m. The pressure vessel is submitted to wind load with the distribution represented in Fig. 14 and an internal pressure of 5.27 MPa. The design variables are 7 thicknesses (Fig. 18) and the objective of the design is the minimization of the volume of shell material considering the maximum displacement and the maximum circumferential stress as constraints. The optimal design is obtained in 7 iterations, 30 function evaluations and 5 gradient evaluations. This design is in agreement with a simplified model used by Mota Soares et al (1987) as shown in Table 9.

8. Conclusions

The results presented show that sensitivity analysis of statical and dynamic constraints of axisymmetric shells are efficiently and accurately obtained using the analytical method here described. When the design variables are thicknesses all the described techniques calculate the response sensitivities with accuracy.

From the observation of results it can be concluded that analytical sensitivities for shape design are more accurate than the semi–analytical ones. Hence analytical sensitivities should be recommended for shape optimization of axisymmetric type structures although they are more difficult to obtain and more expensive in terms of CPU time when compared to the semi–analytical formu-

lation.

The semi–analytical techniques for sensitivities cannot be very accurate and it will require a very small perturbation to obtain acceptable results. However, this perturbation can create problems of numerical stability.

The methods proposed were applied to several design problems and the numerical results show that the frustum–cone finite element used, the algorithms developed to obtained sensitivities and the modified method of feasible directions of ADS make a promising tool to obtain optimal designs for axisymmetric laminate shell structures subject to arbitrary loading.

Acknowledgements

The authors wish to thank for the financial support given by JNICT — Junta Nacional de Investigação Científica e Tecnológica, Proj. C/MPF/531/90 and Proj. STRD/A/TPR/592/92.

References

BARBOSA J. I. (1990) Analytical Sensitivities for Axisymmetric Shells Using Symbolic Manipulator MATHEMATICA, CEMUL Report.

BARTHELEMY B., CHON C. T. AND HAFTKA R. T. (1988) Accuracy problems associated with semi–analytical derivatives of static response, *Journal of Finite Elements in Analysis and Design*, **4**, 249–265.

BERNADOU M., PALMA F. J. AND ROUSSELET B. (1991) Shape optimization of an elastic thin shell under various criteria, *Structural Optimization*, **3**, 1, 7–21.

CHENAIS D. (1987) Shape optimization in shell theory : design sensitivity of the continuous problem, *Engineering Optimization*, **11**, 289–303.

CHENG G. AND LIU Y., (1987) A new computation scheme for sensitivity analysis, *Engineering Optimization*, **12**, 219–234.

HAFTKA R. T. AND KAMAT M. P., (1987) Finite elements in structural design, in C. A. Mota Soares (ed.), *Computer Aided Optimal Design: Structural and Mechanical Systems*, Springer–Verlag, Berlin, 241–270.

KRAUS H., (1967) *Thin Elastic Shells*, John Wiley & Sons, Inc., New York.

MARCELIN J. L. AND TROMPETTE PH., (1988) Optimal Shape Design of Thin Axisymmetric Shells, *Engineering Optimization*, **13**, 108–117.

MEHREZ S. AND ROUSSELET B., (1989) Analysis and optimization of a shell of revolution, in C. A. Brebbia and S. Hernandez (eds.), *Computer Aided Optimum Design of Structures: Applications. Computational Mechanics Publications*, Springer–Verlag, 123-133.

MOTA SOARES C. A., MOTA SOARES C. M. AND MATEUS H., (1987) Optimal design of vertical pressure vessels with supporting cylindrical or conical skirt, *Journal of Engineering Optimization*, **11**, 217–225.

PLAUT R. H., JOHNSON L. W. AND PARBERY R., (1984) Optimal form of shallow shells with circular boundary, *Transactions of the ASME*, **51**, 526–538.

TAYLOR J. E. AND BENDSØE M. P., (1984) An interpretation for min–max structural design problems including a method for relaxing constraints, *Int. J. Solids Structures*, **20**, 4, 301–314.

VANDERPLAATS G. N., (1984) *Numerical Optimization Techniques for Engineering Design*, McGraw–Hill, New York.

VANDERPLAATS G. N., (1987) ADS — A Fortran Program for Automated Design Synthesis, Version 2.01, Engineering Design Optimization, Inc., St. Barbara, California.

ZIENKIEWICZ O. C., (1977) *The Finite Element Method in Engineering Science*, 3rd ed., McGraw–Hill, London.

ZIENKIEWICZ O. C. AND CAMPBELL J. S., (1973) Shape optimization and sequential linear programming, ed. R. H. Gallagher and O. C. Zienkiewicz, *Optimum Structural Design*, Wiley, London.